γ-ray spectroscopy of $^{56}_{26}Fe_{30}$

D. E. Appelbe,[1,*] G. Martínez-Pinedo,[2] R. A. E. Austin,[1] J. A. Cameron,[1] J. Chenkin,[1] T. E. Drake,[3] B. Djerroud,[1] S. Flibotte,[1] D. N. Parker,[1] C. E. Svensson,[4] J. C. Waddington,[1] and D. Ward[4]

[1]*Department of Physics and Astronomy, McMaster University, Hamilton, Ontario, Canada L8S 4M1*

[2]*Institut for Fysik og Astronomi, Århus Universitet, DK-8000 Århus C, Denmark*

[3]*Physics Department, University of Toronto, Toronto, Ontario, Canada M5S 1A7*

[4]*Nuclear Science Division, Lawrence Berkeley National Laboratory, Berkeley, California 94720*

(Received 16 March 2000; published 20 November 2000)

The 8π γ-ray spectrometer has been used to resolve high-spin states in the nucleus ^{56}Fe following the reaction ^{48}Ca(^{13}C,5n)^{56}Fe at a beam energy of 65 MeV. This study has extended the known decay scheme of ^{56}Fe to $J^{\pi}=(13^{+})\hbar$. The experimental decay scheme is compared with theoretical shell model calculations within the pf shell valence space.

PACS number(s): 27.40.+z, 21.60.Cs, 23.20.En, 23.20.Lv

I. INTRODUCTION

The nucleus $^{56}_{26}Fe_{30}$, with two proton holes and two neutron particles outside the $N=Z=28$ shell closures, is the most abundant stable isotope of iron. As such it can be studied using numerous techniques, such as, heavy-ion fusion-evaporation reactions [1,2], β^{-} decay [3], (t,p) reactions [4], and inelastic particle scattering [5]. These methods are all complementary, and have led to a detailed understanding of the level structure at low excitation energies. The most recent studies of the high-spin structure were performed by Sarantites *et al.* [1] and Fromm *et al.* [2] who populated excited states in ^{56}Fe via the ^{46}Ti(^{13}C,2$pn\gamma$)^{56}Fe and the ^{54}Fe(α,2$p\gamma$)^{56}Fe fusion-evaporation reactions, respectively. Sarantites *et al.* determined the decay scheme of ^{56}Fe to $J^{\pi}=8^{+}$, while Fromm *et al*. confirmed the work of Sarantites, extending the level scheme with the addition of several transitions.

Changes in the occupation of the $1f_{7/2}$, $2p_{3/2}$, $1f_{5/2}$, and $2p_{1/2}$ orbitals within the vicinity of the $N=Z=28$ shell closures lead to shape transitions between oblate and prolate deformations. At higher excitation energies well-deformed states based on the occupation of the $1g_{9/2}$ orbital are expected, similar to those observed in ^{62}Zn [7,8]. With such a high density of states and the relatively low excitation energy required to cross the $N=Z=28$ shell closures, neutron-neutron and proton-neutron interactions become important and can play a major role in the observed decay structure of nuclei in this region of the Segré chart. Theoretically, ^{56}Fe has been studied (e.g., Ref. [6]) by the nuclear shell model using the Kuo-Brown interaction (KB) and the surface delta interaction, both forces reproducing the experimental energy levels well. The most recent theoretical treatment of ^{56}Fe at high-spin, that of Vennink and Glaudemans [6], also proposed several bands with enhanced $E2$ transitions. While tentative evidence for one of these bands was observed by both Sarantites [1] and Fromm [2], no evidence for quasirotational bands at higher excitation energy was observed.

In this paper we report upon recent experimental and theoretical results for the nucleus ^{56}Fe. The level scheme has been extended with the observation of several sequences of $M1$ transitions. These results are compared with shell model calculations encompassing the pf valence space and found to be in good agreement.

II. EXPERIMENTAL DETAILS

The reaction ^{48}Ca(^{13}C,5n) has been used to populate high-spin states in the nucleus ^{56}Fe. The 65 MeV ^{13}C beam, provided by the 88 Inch Cyclotron of the Lawrence Berkeley National Laboratory, was incident upon an enriched ^{48}Ca (78%) target. To minimize the oxidation of the calcium, a layer of gold was evaporated on both sides. The target was mounted such that the beam was incident upon 355 μg/cm^2 ^{197}Au, 355 μg/cm^2 ^{48}Ca and exited through a thin layer of ^{197}Au ($\approx$90 μg/cm^2). The resulting γ rays were detected with the 8π spectrometer [9]. A total of 5×10^7 events were recorded in which two or more Compton-suppressed γ rays were detected in the HPGe detectors and at least four elements of the BGO inner ball. The main reaction product was ^{56}Fe (5n). In addition the nuclei ^{57}Fe (4n) and ^{54}Cr (α3n) were populated with 50 and 30 % of the intensity of the ^{56}Fe channel, respectively.

III. RESULTS

These data were sorted offline into a symmetric E_{γ}-E_{γ} coincidence matrix for analysis with the program ESCL8R [10]. An asymmetric matrix to allow the multipolarity of the observed transitions to be determined was also sorted, allowing the asymmetry ratio,

$$R_{asym}=\frac{I_{\gamma_1(\pm37^{\circ}),\gamma_2(\pm79^{\circ})}}{I_{\gamma_1(\pm79^{\circ}),\gamma_2(\pm37^{\circ})}}, \tag{1}$$

to be determined (cf. Refs. [11,12]). Using this method, transition (γ_1) in which $\Delta J=2$ yielded a ratio of 1.0, while those with $\Delta J=1$ gave the value 0.55, when the gating tran-

*Present address: CLRC Daresbury, Keckwick Lane, Daresbury, Warrington WA4 4AD, United Kingdom.

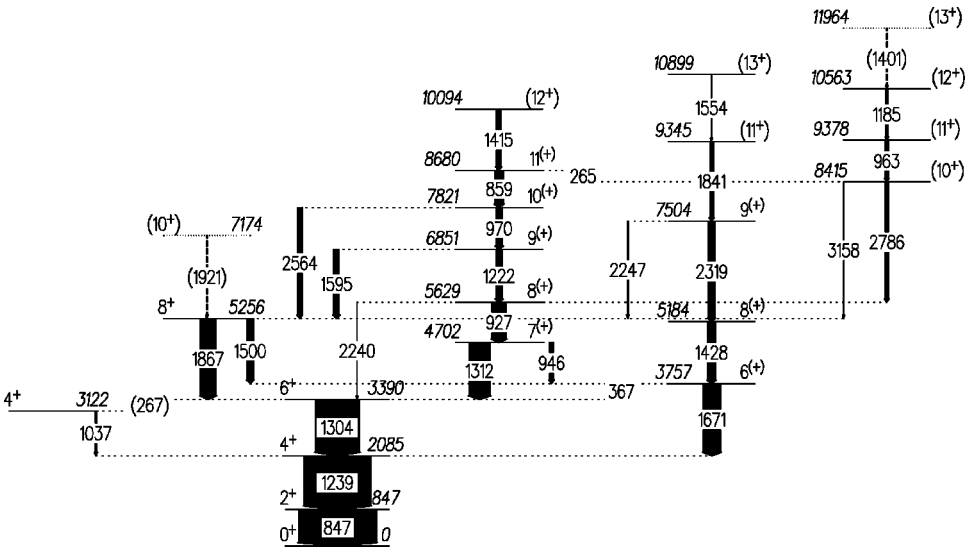

FIG. 1. The level scheme of ^{56}Fe as determined in this experiment. The energies of the excited levels and the γ-ray transitions are given in keV. The widths of the arrows connecting levels are proportional to the relative intensity of the observed transition. Tentative transitions are shown by dashed arrows. Levels with their spin/parity levels in parentheses have uncertain assignment.

TABLE I. The level energies and γ-ray transition properties for the observed transitions in ^{56}Fe. Unassigned spins and parities from the present, or previous works, are listed in parentheses.

E_i (keV)	$J_i^\pi \rightarrow J_f^\pi$	E_γ (keV)	I_γ	R_{asym}
847	$2^+ \rightarrow 0^+$	846.9(3)	100.0(17)	0.90(2)
2085	$4^+ \rightarrow 2^+$	1238.5(3)	85(4)	1.17(2)
3122	$4^+ \rightarrow 4^+$	1037.0(4)	2.27(24)	
3390	$6^+ \rightarrow 4^+$	267.1(4)	0.12(5)	
3390	$6^+ \rightarrow 4^+$	1303.9(3)	57(3)	1.12(2)
3757	$6^{(+)} \rightarrow 6^+$	366.9(3)	4.9(3)	
3757	$6^{(+)} \rightarrow 4^+$	1671.3(3)	22.1(12)	1.09(10)
4702	$7^{(+)} \rightarrow 6^{(+)}$	946.4(3)	4.9(3)	
4702	$7^{(+)} \rightarrow 6^+$	1312.5(3)	27.1(14)	0.78(4)
5184	$8^{(+)} \rightarrow 6^{(+)}$	1427.8(3)	10.2(6)	
5256	$8^+ \rightarrow 6^{(+)}$	1499.5(3)	7.7(4)	
5256	$8^+ \rightarrow 6^+$	1866.8(3)	19.9(10)	0.84(7)
5629	$8^{(+)} \rightarrow 7^{(+)}$	926.6(3)	18.7(10)	0.74(5)
5629	$8^{(+)} \rightarrow 6^+$	2240(3)	0.22(16)	
6851	$9^{(+)} \rightarrow 8^{(+)}$	1221.7(3)	8.4(4)	0.77(10)
6851	$9^{(+)} \rightarrow 8^+$	1595.0(4)	6.9(4)	0.67(18)
7174	$(10^+) \rightarrow 8^+$	1920.9(15)	0.65(15)	
7504	$9^{(+)} \rightarrow 8^+$	2247.1(7)	1.26(16)	
7504	$9^{(+)} \rightarrow 8^{(+)}$	2319.3(3)	7.8(4)	0.55(15)
7821	$10^{(+)} \rightarrow 9^{(+)}$	969.6(3)	8.8(5)	0.76(9)
7821	$10^{(+)} \rightarrow 8^+$	2564.4(4)	5.4(3)	
8415	$(10^+) \rightarrow 8^{(+)}$	2785.7(4)	3.77(25)	
8415	$(10^+) \rightarrow 8^+$	3158.2(14)	0.60(8)	
8680	$11^{(+)} \rightarrow 10^{(+)}$	265.1(3)	1.79(10)	
8680	$11^{(+)} \rightarrow 10^{(+)}$	859.2(3)	10.6(5)	0.56(20)
9345	$(11^+) \rightarrow 9^{(+)}$	1841.1(3)	4.3(3)	
9378	$(11^+) \rightarrow (10^+)$	963.4(3)	3.64(22)	
10094	$(12^+) \rightarrow 11^{(+)}$	1414.5(3)	5.9(3)	
10563	$(12^+) \rightarrow (11^+)$	1184.9(3)	2.47(15)	
10899	$(13^+) \rightarrow (11^+)$	1554.2(7)	0.74(11)	
11964	$(13^+) \rightarrow (12^+)$	1401(3)	1.16(11)	

sition (γ_2), was a stretched quadrupole ($\Delta J=2$). When the gating transition utilized was a stretched dipole ($\Delta J=1$) the resultant R_{asym} ratios for a stretched dipole and stretched quadrupole were 1.0 and 0.5, respectively. The deficiencies of this method are its inability to distinguish between $\Delta J=2$ and $\Delta J=0$ transitions, or to make any assignment as to the degree of mixing present in the transitions.

The level scheme of ^{56}Fe obtained from this analysis is presented in Fig. 1. The experimentally determined properties (energy, intensity, R_{asym}) of the observed γ rays are presented in Table I.

The feeding and decay of all but one of the levels to an excitation energy of 5.63 MeV are found to be in agreement with the level scheme suggested by Fromm *et al.* [2]. The exception is the placement of decays to/from the 5.25 MeV level. This disparity is brought about by a reordering of the 859- and 970-keV transitions, observed to be in coincidence with the 927-keV γ ray. For ease of discussion, the deduced decay scheme of ^{56}Fe has been split into states based on four separate band heads: the ground state, the 4.70 MeV state, the 3.76 MeV state, and the 8.42 state.

States based on the ground state: This sequence of states includes the 0.85-, 2.09-, 3.12-, 3.39-, 5.26-, and 7.17-MeV levels, and accounts for half the previously observed transitions. The decays from these levels are presented in Fig. 2(a), obtained from the sum of gates on the 847- and 1239-keV transitions. Of these states, the 7.17 MeV level that decays by the 1921-keV transition is both new and tentative. The 267-keV transition, observed by both Sarantites and Fromm is also weak, and so denoted as a tentative transition (a stronger 265-keV transition is evident at higher spin). The R_{asym} ratios for these transitions are consistent with that expected for stretched $E2$ transitions, and the angular distributions determined by Sarantites *et al.* [1].

States based on the 4.70-MeV level: This band was previously observed [2] to $J^\pi=10^{(+)}$. The γ rays feeding this state, and the out of the band transitions are previously unreported. Figure 2(b), obtained by a gate on the 1312-keV transition, shows the γ rays associated with the decay of this band. The $\Delta J=1$ nature of these transitions has been in-

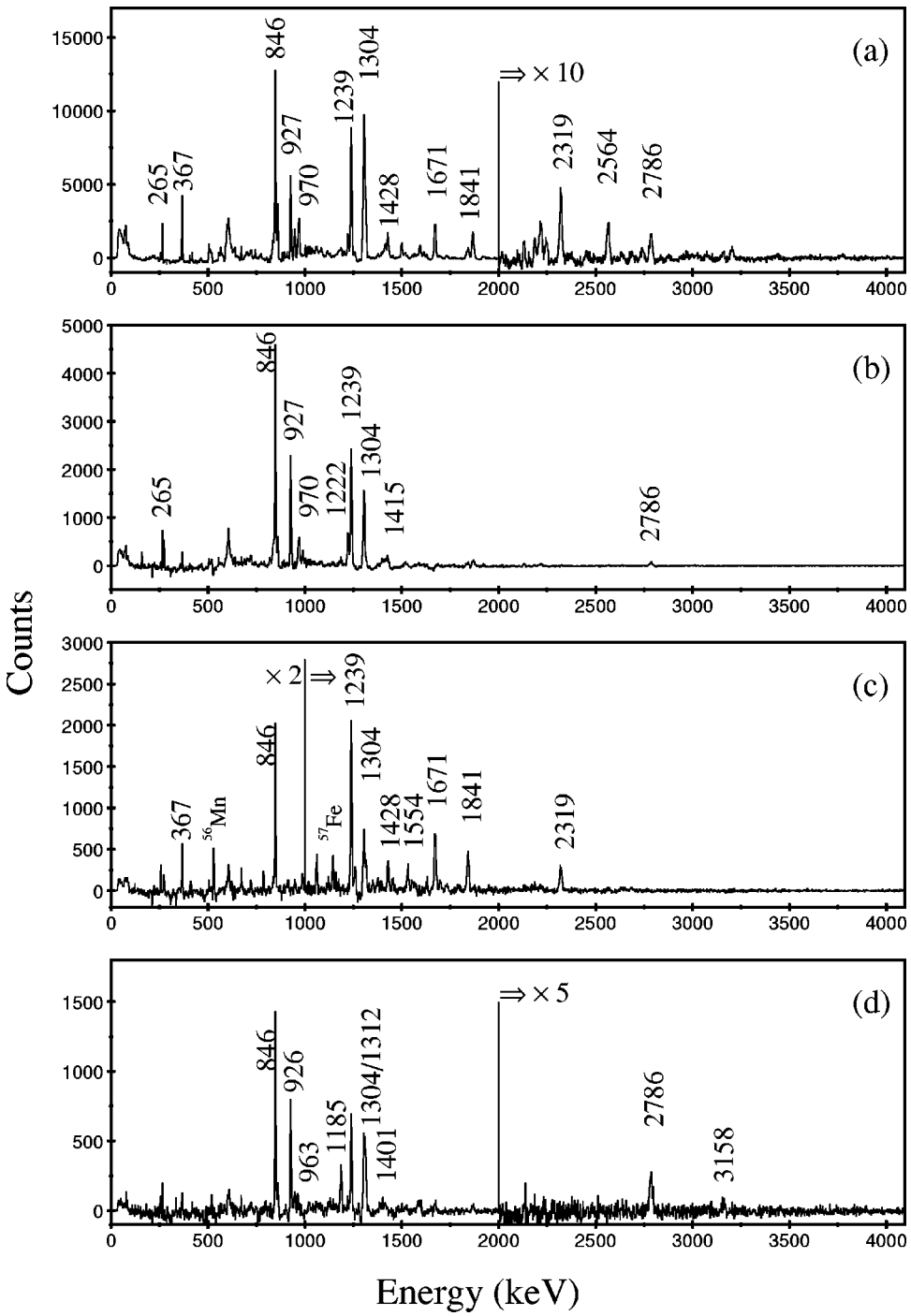

FIG. 2. γ-ray spectra of ^{56}Fe: (a) The sum of gates set on the 847- and 1239-keV transitions. (b) The γ rays in coincidence with the 1312-keV transition. (c) The sum of gates on the 1428- and 2319-keV transitions. (d) Those γ rays in coincidence with the 2786- and 963-keV transitions. The unmarked peaks arise from known contaminants arising from coincidences in ^{57}Fe.

ferred from both the R_{asym} ratios and the decays to other states. For example the 5.63 MeV state decays strongly via the 927-keV transition to the $J^{\pi}=7^{(+)}$ ($E^{*}=4.70$) state and weakly to the $J^{\pi}=6^{+}$ ($E^{*}=3.39$ MeV) state by a 2240-keV transition. This latter decay would be hindered even more than observed if either or both the 1312- and 927-keV transitions were $E2$ as opposed to $M1$ (resulting in a $\lambda=3$ or $\lambda=4$ transition). Similar arguments hold for the $J^{\pi}=9^{(+)}$ 6.85-MeV and $J^{\pi}=10^{(+)}$ 7.82-MeV states which decay via 1595- and 2564-keV transitions, respectively, to the $J^{\pi}=8^{+}$ 5.26-MeV state. At the top of this ''band'' the 10.09 MeV level is observed to decay solely in-band via a 1415-keV γ ray.

States based on the 3.76 MeV level: With the exception of the 367-keV and the 1671-keV γ rays that decay from this band head, all these transitions have been previously unobserved. A spectrum of the in-band transitions based upon this band head is presented in Fig. 2(c). The states in this band, with the exception of the 7.50-MeV level, are observed to decay solely in-band via a sequence of $E2$ transitions. The $J^{\pi}=9^{(+)}$ 7.50-MeV state decays both in-band via a 2319-keV dipole transition and out of band to the $J^{\pi}=8^{+}$ 5.26-MeV state by a 2247-keV dipole transition.

States based on the 8.42 MeV level: Similar to the case of the states based on the 3.76 MeV band head, the levels based on the 8.42 MeV state are only observed to decay purely in

band by a sequence of γ rays that are assumed to be $\Delta J = 1$ transitions. A spectrum is presented in Fig. 2(d) which was obtained by summing gates set on the 2786- and 963-keV γ rays, in which the transitions assigned to this band are marked. The state with the greatest excitation energy [the $J^{\pi}=(13^{+})$ 11.96-MeV level] is very weakly populated and the possibility exists that the observed γ ray is a contaminant from ^{54}Cr. Although no evidence for such a transition was observed in the recent work of Devlin *et al.* [13]. A single gate set on this transition is observed to be in coincidence with yrast transitions in both ^{56}Fe and ^{54}Cr. Accordingly this state is assigned as a tentative level, as is the 1401-keV transition which deexcites it.

IV. DISCUSSION

Nuclei such as $^{56}_{26}\mathrm{Fe}_{30}$, with two protons (holes) and two neutrons (particles) are in close proximity to the doubly magic $^{56}_{28}\mathrm{Ni}_{28}$ nucleus and hence can be considered as shell model nuclei. Such an assumption implies that the observed excited states can be described in terms of particle-hole excitations and has been proved experimentally numerous times (e.g., Ref. [14]) by the observed decays of nuclei such as ^{56,57}Ni and ^{54}Fe.

Theoretically, the most recent calculations of the high-spin structure of ^{56}Fe were performed by Vennink and Glaudemans [6]. These calculations (for $J<8\hbar$) show reasonable agreement with the experimental data obtained from Refs. [1,2]. In addition to the detailed comparison performed at low spin, several predictions for higher spin states ($8 \leqslant J(\hbar) \leqslant 16$) were also presented. These states were calculated assuming three holes in the $f_{7/2}$ shell (the third hole allowed to be either proton *or* neutron). The presence of several sequences of states, with a positive quadrupole moment, connected by $E2$ ($\Delta J=1,2$) transitions was suggested. These microscopic calculations indicated that for states with $J \leqslant 10\hbar$ the third hole in the $f_{7/2}$ orbital is predominantly proton. For the higher spin states, this hole is predominantly neutron. It should be noted that the contribution of the extra hole in the proton $f_{7/2}$ orbital to the wave function of the state increases with spin; varying from $\approx$20% to $\approx$100% (cf. Figs. 9 and 10 of Ref. [6]).

We have performed large scale shell model (SM) calculations within the pf valence space using the shell model code ANTOINE [15]. Our calculation is similar to those presented in Ref. [16] and allows for six holes in the $f_{7/2}$ orbit (the third and successives being either proton or neutron). The results of these calculations are presented in Fig. 3. In Fig. 3 the individual levels are labeled by the notation J_n, where $n=1$ represents the lowest lying level with a spin J. Also shown in this figure are the proton and neutron configurations with the greatest occupancy (given as a percentage). As can be seen from Fig. 3 there exists a good correlation between the experimental and theoretical excitation energies.

As would be expected, the dominant configurations for each of the observed states is based on particle-hole excitations within the $p_{3/2}$, $p_{1/2}$, and $f_{5/2}$ orbitals. It is only at relatively high excitation energies, $E^{*} \geqslant 7.5$ MeV, that a neutron excited across the $N=28$ shell closure plays a dominant

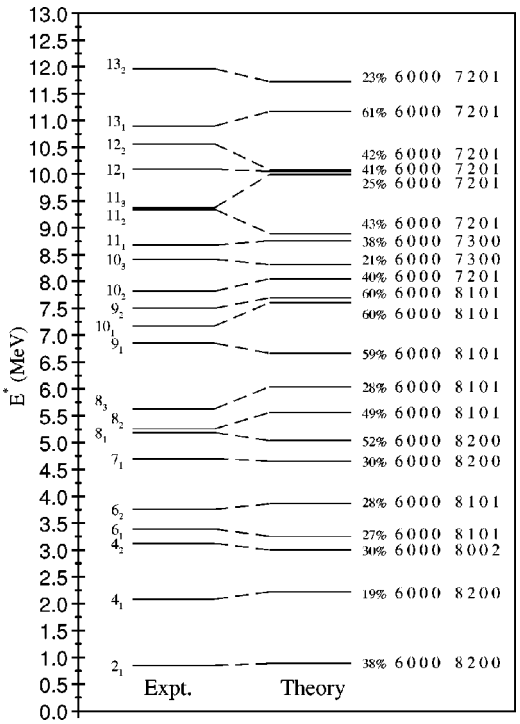

FIG. 3. A comparison between the excitation energies of excited levels in ^{56}Fe. The experimental data are on the left of the figure, while the calculated energies are on the right. Levels of the same J_n are connected by dashed lines. The numbers to the right of the theoretical levels provide the percentage contribution to the wave function of the dominant configuration of each state from the $f_{7/2}$, $p_{3/2}$, $p_{1/2}$, and $f_{5/2}$ proton (first four) and neutron (second four) orbitals, followed by the particle occupation number for these orbitals. The proton configurations for all of these states are primarily based upon the occupation of the $f_{7/2}$ orbital.

role in the configuration of an excited level. This is in contrast to the $N=29$ nucleus ^{53}Cr [12]. In ^{53}Cr the first neutron excitation from the $f_{7/2}$ orbital occurs at $E^{*}=1.54$ MeV. Such an excitation is energetically less favored in the case of ^{56}Fe given the two valence neutrons present outside the $N=28$ shell closure.

In previous studies of ^{56}Fe [1,2,6] it was pointed out that a shape change from prolate to oblate with increasing spin occurs at $J=6\hbar$. In Fig. 4 the calculated spectroscopic quadrupole moment for the observed states in ^{56}Fe has been plotted. To determine which states are prolate and which are oblate the spectroscopic quadrupole moment has to be transformed to the intrinsic quadrupole movement Q_0. These are related by

$$Q_0 = \frac{(J+1)(2J+1)}{3K^2 - J(J+1)} Q_{spec}(J) \qquad (2)$$

thus requiring the K of the band head to be known [17].

Using Eq. (2) we have calculated the intrinsic quadrupole moment for the $10_1 \rightarrow 8_2 \rightarrow 6_1 \rightarrow 4_1 \rightarrow 2_1 \rightarrow 0$ decay sequence and the 6_2 state. This is plotted in the inset of Fig. 4. As can be seen the $6_2 \rightarrow 4_1 \rightarrow 2_1 \rightarrow 0$ sequence is clearly prolate, while the $10_1 \rightarrow 8_2 \rightarrow 6_1$ sequence represents an oblate shape.

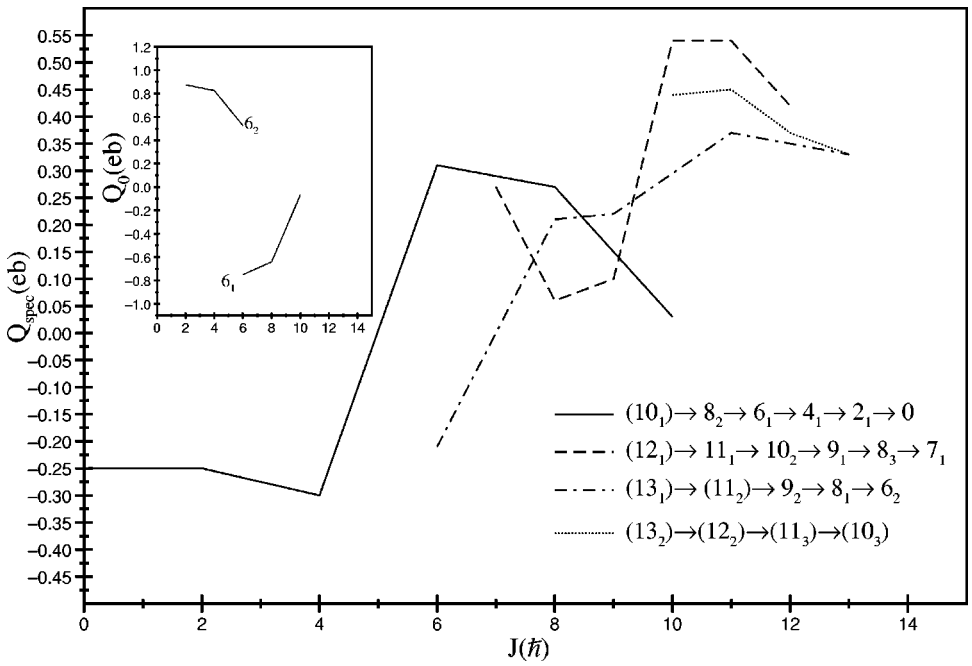

FIG. 4. The theoretically determined spectroscopic quadrupole moments for the four main decay sequences in ^{56}Fe. The inset shows the quadrupole moment that would be measured experimentally for the prolate $6_2\rightarrow 4_1\rightarrow 2_1\rightarrow 0$ and the oblate $10_1\rightarrow 8_2\rightarrow 6_2$ decay sequences.

The prolate-oblate shape change is clearly visible, occurring at $J=6\hbar$ in agreement with the previous publications.

The remaining sequences are calculated to be oblate or near spherical in shape confirming the relatively neutral deformation driving orbitals immediately above the $N=28$ shell closure. Of these sequences those states decaying through the 8.42-MeV level exhibit characteristics most similar to those predicted by Vennink and Glaudemans [6]. Clearly further study of ^{56}Fe is required to confirm these predictions. The good agreement exhibited between the data and theory indicate that these oblate/near spherical states are shell model states as opposed to ''shears-bands,'' which are observed in heavier mass regions [18].

In summary, the level scheme of $^{56}_{26}Fe_{30}$ has been revised and extended to $J^{\pi}=13^{(+)}\hbar$, with the addition of 16 new γ-ray transitions. It has been found that states in ^{56}Fe are well reproduced by pf shell model calculations.

ACKNOWLEDGMENTS

We would like to thank the crew of the 88 Inch Cyclotron for providing the high quality beam, J. Greene (Argonne National Laboratory) for manufacturing our targets, and D. C. Radford for his analysis software [10]. This work has been supported by the Natural Sciences and Engineering Research Council of Canada and by the U.S. DOE. under Contract No. DE-AC03-76SF00098.

[1] D. G. Sarantites, J. Urbon, and L. L. Rutledge, Jr., Phys. Rev. C **14**, 1412 (1976).
[2] H. Fromm, H. V. Klapdor, and P. Herges, J. Phys. G **7**, L109 (1981).
[3] S. Hofmann, Z. Phys. **270**, 133 (1974).
[4] B. L. Cohen and R. Middleton, Phys. Rev. **146**, 748 (1966).
[5] R. De Leo *et al.*, Phys. Rev. C **57**, 1604 (1998).
[6] R. Vennink and P. W. M. Glaudemans, Z. Phys. A **294**, 294 (1980).
[7] C. E. Svensson *et al.*, Phys. Rev. Lett. **80**, 2558 (1998).
[8] C. E. Svensson *et al.*, Phys. Rev. Lett. **79**, 1233 (1997).
[9] J. P. Martin *et al.*, Nucl. Instrum. Methods Phys. Res. A **257**, 301 (1987).
[10] D. C. Radford, Nucl. Instrum. Methods Phys. Res. A **361**, 297 (1995).
[11] S. Pilotte *et al.*, Nucl. Phys. **A514**, 545 (1990).
[12] D. E. Appelbe, J. Sanchez, J. A. Cameron, J. Chenkin, T. E. Drake, B. Djerroud, S. Flibotte, A. Poves, J. C. Waddington, and D. Ward (unpublished).
[13] M. Devlin, D. R. LaFosse, F. Lerma, D. Rudolph, D. G. Sarantites, and P. G. Thirolf, Phys. Rev. C **61**, 017301 (1999).
[14] D. Rudolph, C. C. Baktash, M. J. Brinkman, M. Devlin, H.-Q. Jin, D. R. LaFosse, L. L. Riedinger, D. G. Sarantites, and C.-H. Yu, Eur. Phys. J. A **4**, 115 (1999).
[15] E. Caurier, computer code ANTOINE, IRS Strasbourg, 1989.
[16] E. Caurier, K. Langanke, G Martínez-Pinedo, and F. Nowacki, Nucl. Phys. **A653**, 439 (1999).
[17] A. Bohr and B. Mottelson, *Nuclear Structure* (Benjamin, New York, 1975), Vol II.
[18] Amita, Ashok Kumar Jain, and Balraj Singh, At. Data Nucl. Data Tables **74**, 283 (2000).